

## MEASUREMENTS IN A LIQUID ATOMISER SPRAY USING THE PHASE-DOPPLER PARTICLE ANALYSER

Reçu le 29/01/2000 – Accepté le 30/12/2000

### Abstract

Experiments have been carried out at atmospheric conditions using a water atomiser spray. A phase Doppler anemometry was used to perform the measurements of the droplets size, their velocity and concentration, and photographs were taken. The results showed that the small particles with low turbulence occupied the central core of the jet displaying a Gaussian profile for the axial velocity component. The large particles were deflected towards the outer edges of the jet, due to their higher initial momentum, and displayed relatively high levels of turbulence. The variables measured show that their spatial distributions were nearly symmetrical about the x-axis and although the number density of the droplets is very high in the centred region, most of the pulverised liquid was present in the edges of the spray.

**Key words:** spray – phase Doppler anemometry – turbulence.

### Résumé

Des essais ont été réalisés, dans les conditions atmosphériques, avec un atomiseur d'eau. Les mesures de dimension de gouttelettes, de leur vitesse et de leur concentration par anémométrie à phase Doppler ont permis ainsi avec un support photographique de décrire la structure du jet. Les résultats montrent que les fines gouttelettes occupent la région centrale du jet avec une faible turbulence et un profil Gaussien de leur vitesse axiale. Les grosses particules sont déviées à cause de leur forte inertie initiale vers les bords du jet. La distribution spatiale de chaque grandeur mesurée est presque axialement symétrique et bien que la densité (en nombre) des gouttelettes soit plus élevée dans la région centrale, la plupart du liquide et le maximum de son flux sont éloignés de celle-ci.

**Mots clés:** pulvérisation – anémométrie à phase Doppler – turbulence.

### R. HADEF

Institut de Génie Mécanique  
Centre Universitaire Larbi Ben  
M'Hidi, B.P. 297, 04000  
Oum El Bouaghi (Algérie)

### K. MERKLE

B. LENZE  
University of Karlsruhe  
76128 Deutschland

### ملخص

يقدم هذا البحث نتائج التجارب التي أجريت على مرذاذ للماء. إن مقياس مشخصات قطرات الماء (الحجم، السرعة، الكثافة) باستعمال أشعة الليزر مكن مع التصوير الشمسي من وصف تركيب إنبجاس الماء.

تبين النتائج أن القطرات الصغيرة تحتل المنطقة المركزية باهتياج ضعيف و أن القطرات الكبيرة أنحرفت نحو حافة الانبجاس. التوزيع الفضائي لكل مقدار مقياس تناظري و رغم أن كثافة عدد القطرات مرتفعة في المنطقة الوسطى، توجد أكبر نسبة من الماء بعيدة عن هذه المنطقة.

**كلمات مفتاح:** رذ – قياس السرعة والحجم – اهتياج.

In chemical and certain manufacturing industries, control of a process of a process often requires information on droplets size, number density and the trajectory of individual droplets. This information is particularly useful in a certain number of processes such as powder atomisation, spray drying, cooling towers, agricultural and industrial spraying, fire extinguishers [1]. Since these values serve to broadly segregate different atomizer designs or process, spatially resolved information (droplet size, number density, velocity, etc.) needs to be obtained in order to develop a full understanding of the processes that occur in spray (collision, coalescence, break up, etc.) [2].

Although in recent years the phase Doppler anemometer (PDA) instrumentation has become a powerful tool for spray characterisation with respect to the droplet size and velocity, great errors have been reported. Such errors have been attributed to several different sources including improperly sized droplets [3, 4], non-uniform reference area for the measurement [5], or incorrect particle counts due to poor signal validation. More recently, considerable effort has been produced in order to minimise or compensate for such errors, and thus increase the reliability of the PDA technique [6].

This paper presents the results of an experimental investigation carried out using a dual PDA that combines a conventional PDA and a planar PDA [7]. Each PDA uses a different laser wavelength and their combination (the so-called dual PDA) permits the measurement of the

mean as well as the root-mean-square of the two velocity components and the size of the particles. This technique is applied to characterise and find out the geometrical performance of a pressurised water nozzle, which may be applied for soaking, salted water by means of flashing [8].

### THE PHASE DOPPLER SIZE AND VELOCITY MEASUREMENT TECHNIQUE

The PDA technique permits the simultaneous measurement of both particle size and velocity independently of the laser beam intensity and its attenuation due to the flow turbidity [9]. As in the well-know laser Doppler velocimetry (LDV) [10], this technique uses two monochromatic and coherent beams focused to obtain a beam intersection. In this intersection, planar interference fringes are produced parallel to each other and separated by a distance known as the fringe spacing  $\delta$ :

$$\delta = \frac{\lambda}{2 \sin \frac{\theta}{2}}$$

where  $\lambda$  is the wavelength of the laser light and  $\theta$  is the intersection angle between the laser beams. Although LDV measurements require only one photomultiplier tube (PMT) to detect the Doppler frequency ( $F_D$ ) of the light scattered by a particle passing through the fringes, the phase Doppler technique needs two PMT in order to detect the Doppler burst (Fig.1), but with a typical time difference  $\Delta t$ , relating to the particle velocity and to the curvature of its surface (the diameter of a spherical particle). The velocity component of the particle,  $U_{\perp}$ , perpendicular to the fringes, can be deduced from the Doppler frequency  $F_D$  ( $= T_D^{-1}$ ) measured by a counter through the relation:

$$U_{\perp} = F_D \delta$$

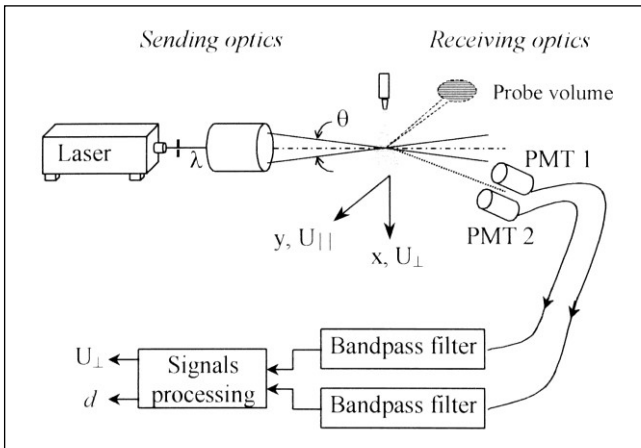


**Figure 1:** Phase-Doppler measurement system.

A Doppler burst signal will be produced by each detector but with a phase shift between them, as illustrated in figure 2. The signals in this figure have been high-pass filtered to remove the pedestal component. The phase shift,  $\Delta\phi$ , is then determined by measuring the time,  $\Delta t$ , between

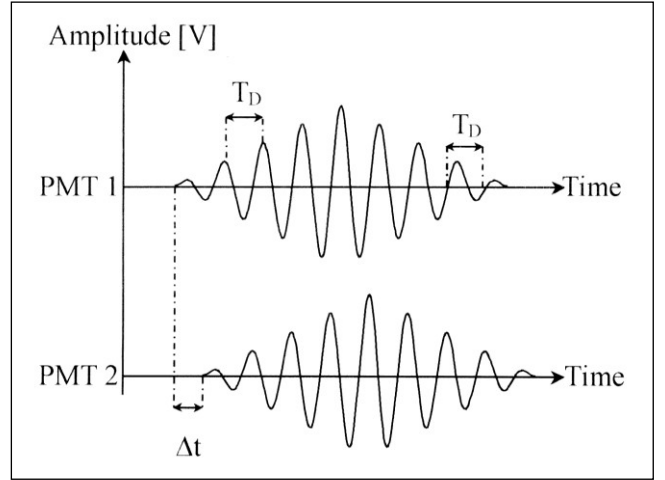


**Figure 2:** High-pass filtered Doppler burst signals illustrating the phase shift between detectors.

the zero crossings of the signals from PMT 1 and 2 and dividing by the measured Doppler period by the relation:

$$\Delta\phi = \frac{2\pi}{T_D} \Delta t$$

where the measurements are averaged over all the cycles in the Doppler burst signal. Measurements of the phase shift are then related to the drop size using the linear relationship [11]:

$$d = \frac{1}{2\pi b} \left( \frac{\lambda}{n_c} \right) \Delta\phi$$

where  $n_c$  is the refractive index of the continuous phase (air) and  $b$  is a function of the geometrical arrangement of the experimental set-up and of refractive index of the dispersed phase [12].

In this investigation, the dual PDA is used [13]. It is based on a specifically designed PDA receiving recently developed optics [14]. Owing to the shortcomings of conventional PDA systems, the dual PDA was developed to improve the measurement accuracy of mass flux and concentration. Its concept is to make two independent size measurements using both the conventional and the planer PDAs. Each system would yield the same result only if the refractively scattered light is received at the photodetector and if the particle is spherical. If however the reflectively scattered light dominates because of either slit effect or the trajectory, each system will yield a different size and they will no longer agree. This redundancy can therefore be used as a validation criterion in order to avoid the slit effect [15] and the trajectory effect [16].

### EXPERIMENT

The phase-Doppler system used for the present experiments is shown in figure 3. A light source employed is an argon-ion laser with a component separation based on colour (514.5nm: axial velocity component, 488nm: radial velocity component). Bragg cell was used to split the light from the laser (typical operating output: 0.2W) in two beams with one beam frequency-shifted at 40 MHz to avoid

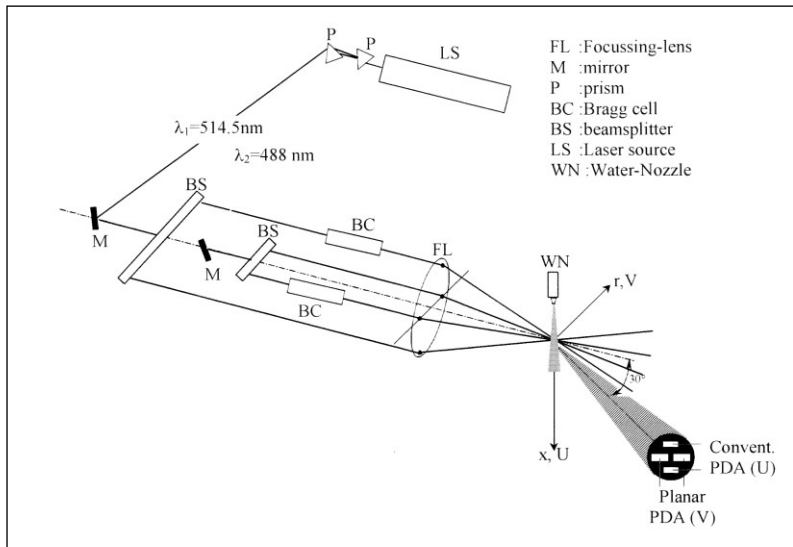


**Figure 3:** Optical arrangement of the dual-PDA measurements.

directional ambiguity and to measure the velocity fluctuation. The receiver at 30° off-axis forward and refraction scattering mode with 400-mm focal length lens detected the scattering light. The measurement volume is approximately 53 μm in diameter and 2 mm in length. But due to the lens on the receiving probe a piece of only 0.2-mm is "cut out" of the measurement volume and projected on the receiving fibres that transport the signal to the photomultipliers. The injector spray was fixed while the optical set-up (transmitting and receiving) was mounted on a stepper-motor driven traversing system. By means of this, movement in the axial and horizontal planes is allowed, thus enabling the measurement of radial profiles of scattered light intensity at different axial positions. In the measurements of mean quantities at each given location, 10000 samples were taken, except in some regions where the data rate became very low and therefore the sample size was restricted to around 1000 drops to avoid long run times.

The optic transmission and reception parameters used in this study are given in table 1. A pressure-atomizing injector provides a cone water spray which is vertically injected downwards from the nozzle exit. The liquid flow rate in the experiment described in this paper was 0.845 l/h. and is introduced through a 0.21mm diameter orifice.

Transmission optics		
	Convent.	Planar
Laser wavelength (nm)	514.5	488
Beam separation (mm)	40	40
Focal length (mm)	450	450
Frequency shift (MHz)	40	40
Fringe spacing (μm)	2.329	2.209
Receiving optics		
Off-axis angle (°)		30
Focal length (mm)		400
Aperture mask		Small
Phase factor conventional (°/μm)	7.7801	
Phase factor planar (°/μm)	2.7385	

**Table 1:** Configuration of the dual-PDA.

For each particle crossing the measurement volume, the Doppler frequency and phase difference are measured, and the two velocity components (axial and radial), their root-mean-square and diameter are stored on a personal computer. Data analysis is performed off-line and provides size and velocity distributions, as well as the size-velocity correlations and the particle concentration. For processing of the Doppler bursts, a covariance signal processor was used. This device determines signal frequency and phase difference for both the conventional PDA and the planar PDA. This processor performs burst detection and the initial signal validation by analogy, on-line determination of the signal-to-noise ratio.

## RESULTS AND DISCUSSION

The main objective of the present research is the determination of the flow field structure formed by the disintegration of the liquid into droplets. The size distributions and the mean diameters at each point were based on 10 000 measurements, except in some region where the data rate became very low and therefore the sample size was restricted to around 1000 drops to avoid long run times. Droplet velocity was obtained in 50 size ranges of 5 μm. In this temporal distribution, the number of particles in each size range depends on this size. The diameters used to characterise the spray are the arithmetic mean diameter ( $D_{10}$ ) and the Sauter mean diameter, SMD, ( $D_{32}$ ) calculated respectively as:

$$D_{10} = \frac{\sum_{i=1}^I n_i d_i}{\sum_{i=1}^I n_i} \quad D_{32} = \frac{\sum_{i=1}^I n_i d_i^3}{\sum_{i=1}^I n_i d_i^2}$$

where  $n_i$  is the "weighted number" of particles in the size range of diameter  $d_i$  and  $I$  is the number of size ranges (equal to 50).

Figure 4 shows the probability density function (pdf's), or histogram, of the droplet diameter at  $x=10$ mm. It presents a shift in the size distribution in the radial direction. It is narrow monomodal at all the positions (of varying mean diameter at different positions), and possesses a maximum close to the mean diameter value. In the inner region of the spray a sharp peak in a small diameter range is seen, whereas in the outer the probabilities of small droplets decrease since the larger particles begin to appear. This is a very typical size distribution for air-pressurized atomizer sprays in which the small drops are located in the center region and the SMD increases gradually along with the increase in radial distance. Larger drops possess higher initial momentum, which allows them to penetrate farther and to wider distances (Fig. 5). In general, the number density distribution is nearly uniform in the centred region of the spray and then gradually decreases with radial

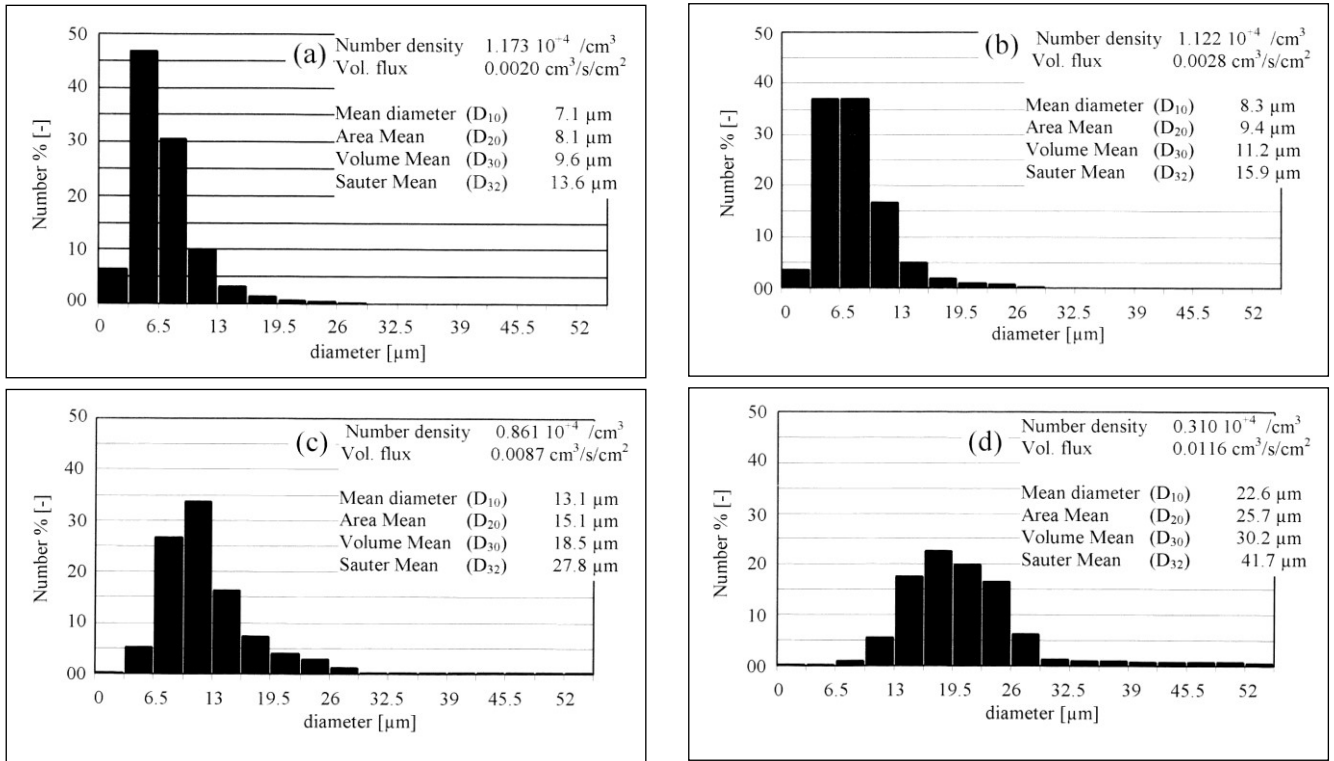


**Figure 4:** Droplet size distributions obtained for  $x = 10\text{mm}$  at  $r = 0, 2, 4$  and  $8 \text{ mm}$ .

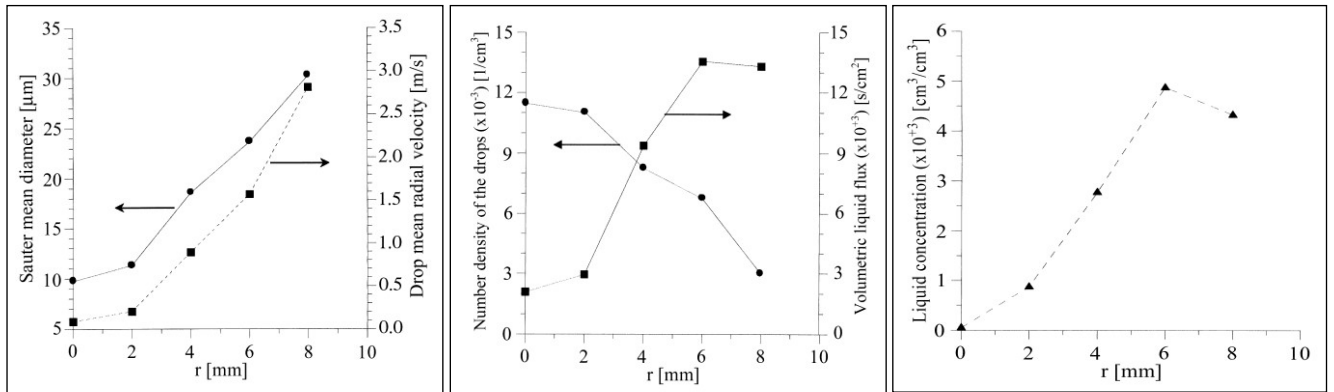


**Figure 5:** Variation of SMD and mean radial velocity of the drops with radial position measured at  $x=10\text{mm}$ .

**Figure 6.a:** Variation of droplet number density and liquid flux with radial position measured at  $x=10\text{mm}$ .

**Figure 6.b:** Variation of pulverised liquid concentration with radial position measured at  $x=10\text{mm}$ .

distance to zero at the spray boundary (Fig. 6.a). Liquid flux measurements for spray are also reported in the same figure and it is noted that the variation of liquid flux is closely associated with droplet size change. It increases with the radial distance to a maximum value and then decreases toward the outer edges of the spray. The relative increase in the number of large drops (possessing higher velocity) contributes to the increase in liquid flux. In the figure 6.b, the results are presented in the form of the liquid concentration instead of droplet number density, because this quantity gives a better indication of the liquid present in the flow. It was estimated by the number density of all the measured droplets ( $N$ ) and the SMD as :

$$C = N \frac{\pi}{6} (D_{30})^3$$

Its shape is also closely associated with the liquid flux change.

Figure 7 shows the radial variation in  $D_{10}$  for four values of the distance to the injector ( $x=10\text{mm}, 15\text{mm}, 20\text{mm}$  and  $25\text{mm}$ ). It can be seen that the central core is occupied by the smallest particles of approximately  $7 \mu\text{m}$  in diameter. By moving from the central core, one may find more important particles, which may reach diameter values of  $40\mu\text{m}$ , and this phenomenon is the same on all planes. Indeed, important particles are given more impulse at their exit and thus are much deviated from the axial direction. However, moving away in the vertical direction leads to finding less important particles. Within these two directions (horizontal and vertical), the loss of the initial momentum is mainly due to the action of air. This latter favours particle

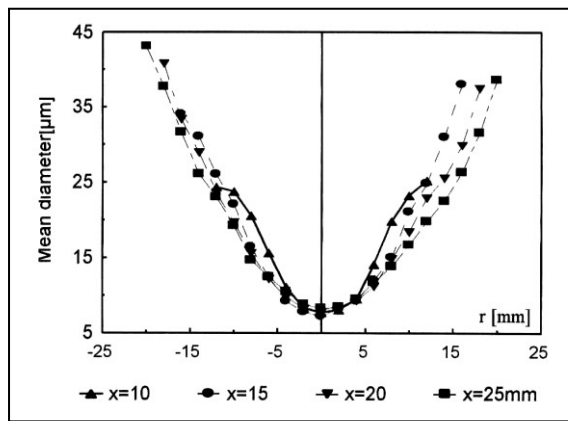


Figure 7: Radial profiles of the mean droplets diameter.

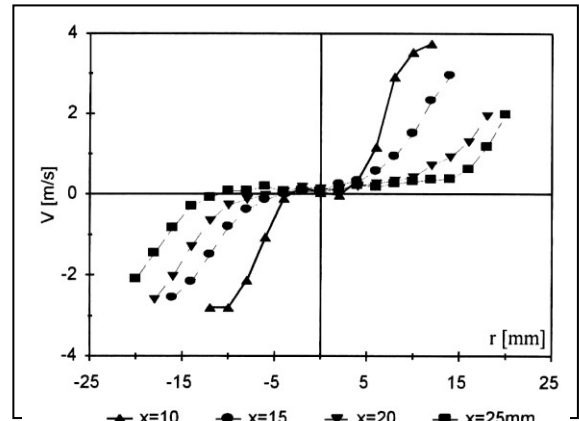


Figure 10: Radial profiles of the mean radial velocity of the droplets.

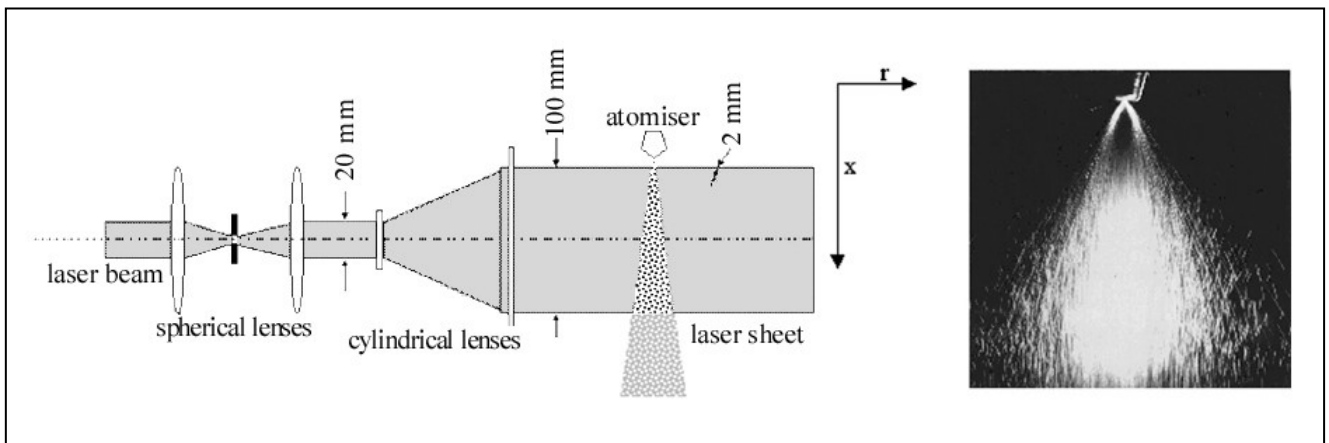


Figure 8: Vertical cross-sectional view of the spray with the laser sheet beam.

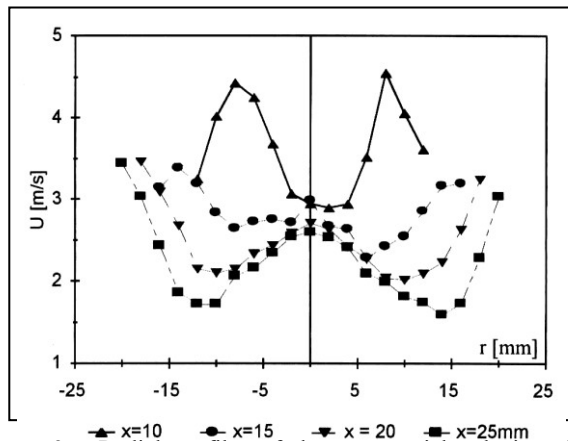


Figure 9: Radial profiles of the mean axial velocity of the droplets.

collisions leading to the constitution of bigger particles thus the increase of the mean diameter and the decrease of the number density of the droplets. A laser sheet beam was used to examine the internal features of the spray. Illumination of the spray with the sheet beam passing vertically through the center line cross section revealed that droplets are concentrated along the central core of the spray and allowed the determination of the jet half-angle cone value to be 42°

(Fig. 8). A much higher number density is observed in the central core region where smaller drops are located.

A two dimensional representation of the mean velocity field (Fig. 9 and 10) and its fluctuation components (Fig. 11 and 12) indicates the formation of two different regions.

In the internal region, the radial distribution of the mean axial velocity was Gaussian in form with the maximum velocity on the axis of the jet, displaying a uniform profile of its fluctuation. On the other hand, the radial velocity component is close to zero and the distribution of its fluctuation is similar to the axial velocity component one. In the secondary region, the turbulence is anisotropic and all the mean variables values ( $U, V, u', v'$ ) increase subject to the bigger particles.

This almost symmetrical structure begins to appear at a distance of 12mm from the exit. Upstream of this station, the axial velocity and its fluctuation show a flat profile with two individuals maxima. They represent the limit of the potential core following the recirculation zone. Indeed, negative values for the axial velocity have been measured in a narrow region. In this case, the concentration radial profile is identical to that of the axial velocity without any influence on the diameter distribution, and the jet takes the proper form illustrated in the figure 13.

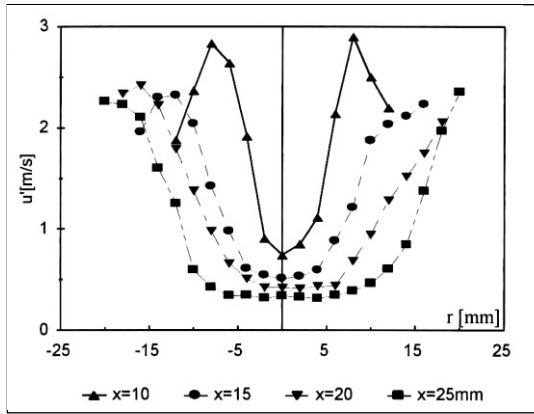


**Figure 11:** Radial profiles of the rms of the mean axial velocity of the droplets.

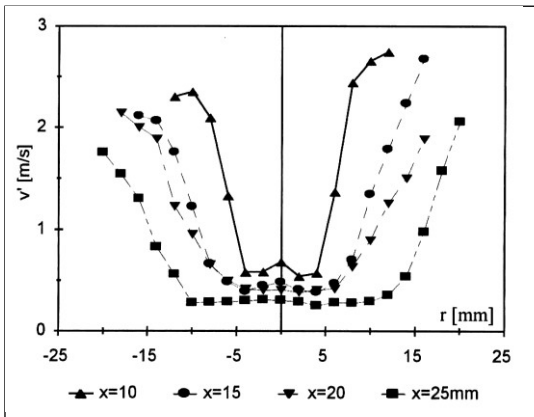


**Figure 12:** Radial profiles of the rms of the mean radial velocity of the droplets.

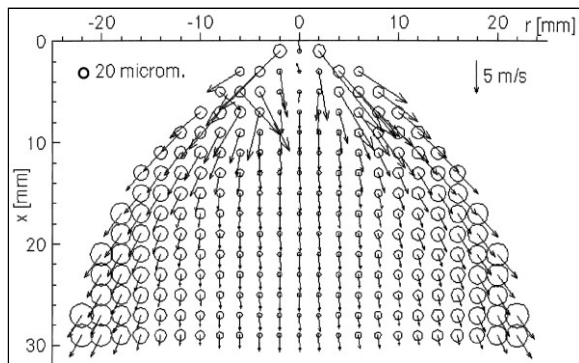


**Figure 13:** Mean field velocity and size distributions of the droplets in the flow.

**CONCLUSION**

The phase-Doppler anemometer has been applied to the local measurement of the velocity and size of droplets in water spray. A quasi-symmetrical profile of the jet has been found (fig. 12). It presents a central core occupied by the small particles having a Gaussian profile with relatively weak turbulence intensity, and surrounded by larger particles with a high degree of anisotropic turbulence. The measured quantities presented a spatial distribution, which was nearly symmetrical about the x-axis and although the number density of the droplets is very high in the center

region, most quantity of the pulverised liquid was present in the edges of the spray.

*Acknowledgements-* We are grateful to the Bundesministerium für Bildung, Wissenschaft, Forschung und Technologie (BMBF-Deutschland) for financial support under Keromix Program. The first author is pleased to acknowledge the Deutscher Akademischer Austauschdienst for the provision of the research fellowship.

**REFERENCES**

- [1]- Bauckhage K., Fritsching U. and Schulte G., "Spray, Erfassung von Sprühvorgängen und Techniken der Fluidzerstäubung", *Spray '96*, Universität Bremen (1996).
- [2]- Qian J. and Law C. K., *AIAA 94-0681, 32<sup>nd</sup> Aerospace Sciences Meeting*, Jan. (1994).
- [3]- Aizu M., Durst F., Gréhan G., Onofri F., Xu T-H., "PDA System without Gaussian Beam Defects", *The 3<sup>rd</sup> International Congress on Optical Particle Sizing*, August 23-26, Yokohama, Japan (1993), pp 461-470.
- [4]- Gréhan G., Gouesbet G., Naqwi A. and Durst F., "Evaluation of a Phase Doppler System using Generalized Lorenz-Mie Theory", *Int. Conf. on Multiphase Flows*, Tsukuba, Japan (1991), pp. 291-296.
- [5]- Saffman M., "Automatic Calibration of Measuring Volume Size", *Appl. Opt.*, 26, (1987), pp. 592-597.
- [6]- HadeF R., Merkle K., Lenze B. and Leuckel W., "An experimental study of air blast atomizer spray flames", *Journal of the Institute of Energy*, N° 73, (2000), pp. 50-55.
- [7]- HadeF R., Merkle K., Lenze B., Leuckel W., "Untersuchung zum Stabilitätsverhalten einer mit Kerosin betriebenen Air-Blast-Zertauberdüse", *The 33<sup>rd</sup> Internationales Seminar für Forschung und Lehre in Chemieingenieurwesenn*, Karlsruhe, Germany (1997) pp.72-82.
- [8]- Safi M.J., "The Solar Pound in Tunis", *European Desalination Society Newsletter*, Issue 7 (1999), pp. 7-8.
- [9]- Hardalupas Y. and Taylor A. M. K. P., "The Identification of LDA Seeding Particles by the Phase-Doppler Technique" *Experiments in Fluids*, Vol. 6, (1988), pp. 137-140.
- [10]- Haddad A., Khezzer L., Benhamza M. H., HadeF R. et Satha H., "La vélocimétrie laser et ses applications en hydrodynamique", *Séminaire National sur le Laser et ses Applications (SENALAP'99)*, Alger (1999), pp. 265-268.
- [11]- Bachalo W.D. and Houser M.J., "Phase-Doppler Spray Analyser for Simultaneous Measurements of Drop Size and Velocity Distributions", *Optical Engineering*, Vol. 23, (1984), pp. 583-590.
- [12]- Bauckhage K., "Anwendungstechnische Aspekte zur Phasen-Doppler-Methode in der Partikelsmeßtechnik", *Technisches Messen*, 56, (1989), pp. 22-27.
- [13]- Merkle K., Ament A., Lenze B., Leuckel W. and HadeF R., "Untersuchung zum Stabilitätsverhalten einer Air-Blast-Zertauberdüse", *VDI-Berichte*, N°1492 (1999), pp.449-454.
- [14]- HadeF R., Merkle K., Lenze B. and Leuckel W., "Flow measurements in a liquid fuel flame", *The 26<sup>th</sup> Congress of AICHEMIA 2000*, Frankfurt am Main (2000).
- [15]- Durst F., Tropea C. and Xu T-H., "The Slit Effect in Phase Doppler Anemometry", *2<sup>nd</sup> Int. Conf. on Fluid Dyn. Meas. an its Appl.*, Beijing (1994), pp. 38-43.
- [16]- Willmann M., Eigenmann L., Wittig S. and Hirleman E. D. "Experimental Investigations on the Effects of Trajectory dependent Scattering on Phase Doppler Particle Sizing with a Standard Instrument", *7<sup>th</sup> Int. Symp. on Appl. of Laser Techniques to Fluid Mechanics*, Lisbon, Portugal (1994), pp. 18.1.1-18.1.7. □